s-d exchange interaction induced magnetoresistance in magnetic ZnO

Qingyu Xu,* Lars Hartmann, and Heidemarie Schmidt
Forschungszentrum Dresden-Rossendorf, Institut für Ionenstrahlphysik und Materialforschung, Bautzner Landstraße 128, 01328 Dresden, Germany

Holger Hochmuth, Michael Lorenz, Daniel Spemann, and Marius Grundmann
Universität Leipzig, Fakultät für Physik und Geowissenschaften, Institut für Experimentelle Physik II, Linnéstrasse 5, D-04103 Leipzig, Germany

(Received 26 June 2007; published 23 October 2007)

The magnetoresistance (MR) effect in Co-doped ZnO films prepared by pulsed laser deposition on *a*-plane sapphire substrates with electron concentration at 5 K ranging from 8.3×10^{17} cm^{-3} to 9.9×10^{19} cm^{-3} has been studied experimentally and theoretically. A large positive MR of 124% has been observed in the film with the lowest electron concentration of 8.3×10^{17} cm^{-3}, while only a negative MR of −1.9% was observed in the film with an electron concentration of 9.9×10^{19} cm^{-3} at 5 K. The positive MR is attributed to the quantum correction on the conductivity due to the *s-d* exchange interaction induced spin splitting of the conduction band. The negative MR is attributed to the magnetic field suppressed weak localization. The presented modeling of superimposed positive and negative MR well agrees with the experimentally observed MR and hints at the physical origin of MR in Co-doped ZnO.

DOI: 10.1103/PhysRevB.76.134417 PACS number(s): 75.50.Pp, 75.47.De, 75.30.Et, 73.20.Fz

There is great interest in ZnO due to its optoelectronic applications owing to its direct wide band gap ($E_g\sim3.3$ eV).[1] After the theoretical predication of room-temperature ferromagnetism in 5% Mn-doped ZnO,[2] much work has been done on magnetic ZnO for future applications in spintronics. Besides the abundant experimental work and results on the magnetic properties of doped ZnO,[3,4] the magnetotransport behavior, including magnetoresistance (MR) and the anomalous Hall effect (AHE), was also studied in ZnO and magnetic doped ZnO.[5–10] In ZnO and nonmagnetic ion doped ZnO—for example, Ga-doped ZnO—negative MR at low field and positive MR at high field was observed. Large positive MR was observed at low field in magnetic ion doped (Mn, Co, etc.) ZnO. The MR in magnetic ZnO depends in a complicated manner on temperature and electron concentration. Recently, we reported that the MR in Co-doped ZnO strongly depends on the electron concentration.[7,8] The positive MR in Mn-doped ZnO has been modeled by accounting for the quantum correction of *s-d* spin splitting on the disorder-modified electron-electron interaction, while the mechanism of the large negative MR at high field is still not clear.[6] However, at low temperature the large field MR behavior in Co-doped ZnO and Mn-doped ZnO are distinct namely only small high field negative MR has been observed in Co-doped ZnO.[8] In this paper, we extend the modeling of *s-d* spin splitting on the disorder-modified electron-electron interaction to explain the positive MR in Co-doped ZnO in weak localization. Furthermore, we model the negative MR in Co-doped ZnO by the field-induced suppression of weak localization[11] and also apply our model to Co-doped ZnO in the strongly localized regime.

Co-doped ZnO films were grown from $Zn_{0.945}Co_{0.05}Al_{0.005}O$ ceramic targets on 10×10 mm^2 *a*-plane sapphire substrates by pulsed laser deposition (PLD) using a KrF excimer laser under different substrate temperatures and oxygen pressures.[7,8] The film thickness was controlled by the number of laser pulses with an energy density of 2 J cm^{-2} and *ex situ* determined by modeling spectral ellipsometry data measured in the energy range of 1–4 eV.[12] The resulting composition of the films was determined by combined Rutherford backscattering spectrometry (RBS) and particle-induced x-ray emission (PIXE) measurements. Due to the underlying Al_2O_3 substrate, the Al content in the films could not be determined. Four samples, labeled *A*, *B*, *C*, and *D*, with electron concentration ranging from 9.9×10^{19} cm^{-3} to 8.3×10^{17} cm^{-3} were selected for the MR study. Their properties are listed in Table I. The crystal structure of the films was characterized by x-ray diffraction measurements with θ-2θ scans using a Cu $K\alpha$ source. Only (002) and (004) peaks of wurtzite ZnO were observed, indicating the highly *c*-axis-oriented magnetic ZnO films without any visible impurities. The structure of the films was also studied by transmission electron microscopy (TEM). No impurities were observed. The Co^{2+} distribution was uniform in the film as observed by electron energy loss microscopy (EELS) and elemental mapping.[8,13] Magnetotransport measurements with the field applied parallel to the *c* axis of the films (perpendicular to film surface) were performed in van der Pauw configuration. Fields up to 6 T were applied over a wide

TABLE I. The PLD deposition parameters (oxygen partial pressure P_{O2}, substrate temperature T_s), Co concentration x in the deposited $Zn_{1-x}Co_xO$ films, film thickness t, electron concentration n, and mobility μ at 5 K.

Sample	x	P_{O2} (mbar)	t (nm)	T_s (°C)	n (5 K) (cm^{-3})	μ (5 K) (cm^2 V^{-1} s^{-1})
A	0.07	4×10^{-5}	26.5	350	9.9×10^{19}	17.5
B	0.1	4×10^{-5}	689	650	1.7×10^{19}	41.1
C	0.098	4×10^{-5}	261	610	5.1×10^{18}	13.9
D	0.1	3×10^{-3}	685	650	8.3×10^{17}	1.2

TABLE II. Values of $k_F l$ of fitting parameters x_{eff} and F_σ for positive MR and of fitting parameter L_{Th} for negative MR. For the high-temperature negative MR, only L_{Th} was determined from the fitting. The number of digits reported is determined by the accuracy of the modeling.

Sample	T (K)	$k_F l$	x_{eff}	F_σ	L_{Th} (nm)
A	5	2.36	0.008	0.62	29.0
	20				20.0
	50				18.3
	200				5.45
B	5	1.71	0.035	0.10896	60.0
	20		0.09	0.15371	21.0
	50		0.09	0.47801	11.7
	290				2.3
C	5	0.27	0.035	0.025	9.0
	20		0.07	0.074	8.0
	50		0.09	0.203	6.9
	200				2.15
D	5	0.0065	0.06	0.00015	2.3
	20		0.09	0.00536	2.3
	50		0.09	0.0883	5.8
	100				2.15

temperature range from 5 K to 290 K. The type of the conducting carriers was confirmed to be *n*-type by Hall measurements for all the samples.

The product of the Fermi wave vector k_F and mean free path l can be calculated with equation $k_F l = \hbar(3\pi^2)^{2/3}/(e^2 \rho n^{1/3})$, where $\hbar$ is the Planck constant, e the electron charge, ρ the resistivity, and n the electron concentration.[14] $k_F l$ values of the samples calculated with n and ρ at 5 K increase with increasing electron concentration, as shown in Table II. Systems with $k_F l > 1$ will lie in the weakly localized regime.[6] For comparison, Fig. 1 shows the typical MR (defined as $(R[H]-R[0])\times 100\%/R[0]$) curves

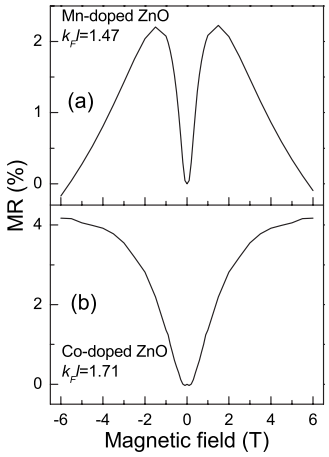

FIG. 1. Field-dependent MR curves for (a) Mn-doped ZnO and (b) Co-doped ZnO at 5 K in weakly localized regime with similar $k_F l > 1$.

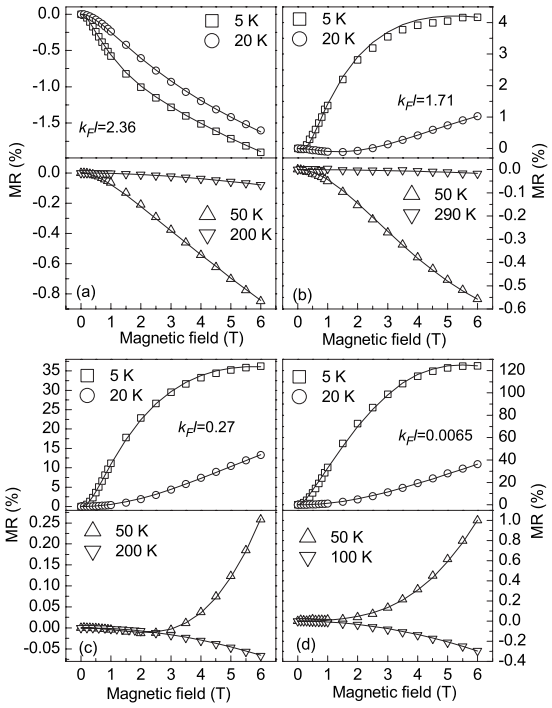

FIG. 2. The magnetoresistance vs magnetic field (open symbols) for (a) sample *A*, (b) sample *B*, (c) sample *C*, and (d) sample *D* at different temperatures. The solid lines are the fitting curves using three-dimensional equations for (b), (c), and (d). For (a), two-dimensional equations were used for 5 K and 20 K, and three-dimensional equations were used for 50 K and 200 K.

at 5 K for a Mn-doped ZnO with $k_F l \approx 1.47$ and Co-doped ZnO with $k_F l \approx 1.71$—i.e., in the weakly localized regime. Both films show clearly the positive MR at low fields. However, Mn-doped ZnO shows strong negative MR at high field, while Co-doped ZnO only shows weak negative MR.

Figure 2 shows the MR behavior in Co-doped ZnO in dependence on electron concentration and temperature. Compared with the critical electron concentration $n_c = 4\times 10^{19}$ cm^{-3} determined from the temperature-dependent resistance and MR behavior,[7] at low temperature negative MR ($n > n_c$) changes to large positive MR ($n < n_c$). The positive MR decreases drastically with increasing temperature, and only negligible negative MR can be observed above 50 K.

In magnetic doped ZnO, the positive MR is related with the quantum corrections to the conductivity due to the influence of the spin splitting of the conduction band on the electron-electron interaction.[6,11,15] Currently, for negative MR, the underlying physical origin is much debated. We previously observed negative MR in Ti-, Cu-, and Nd-doped ZnO and modeled it by considering the magnetic scattering of the conduction electrons by isolated magnetic ions, as proposed by Csontos *et al.*[16] We applied the model of Csontos *et al.* to Co-doped ZnO and observed that above 50 K the negative MR in Co-doped ZnO is not mainly influenced by magnetic impurity scattering. For semiconductors in the weak localization region, the field suppression of weak localization is a possible origin for the small negative MR,[11]

which has been applied to explain the small negative MR in Co-doped ZnO. In the following, the positive MR due to the quantum correction of *s-d* spin splitting on the disorder-modified electron-electron interaction and negative MR due to the field suppression of weak localization are combined together to model MR in Co-doped ZnO.

For the positive MR, the change of conductivity can be modeled as follows:[11]

$$\Delta\sigma_P(H,T) = \sigma(H,T) - \sigma(0,T) = -\frac{e^2}{\hbar}\frac{F_\sigma}{4\pi^2}g_2(\beta) \tag{1}$$

$$= \frac{e^2}{\hbar}\frac{F_\sigma}{4\pi^2}\sqrt{\frac{kT}{2\hbar D}}g_3(\beta) \tag{2}$$

for two and three dimensions, respectively, with F_σ the screening parameter for the Coulomb interaction ranging between 0 and 1, and

$$g_2(\beta) = \int_0^\infty d\Omega \frac{d^2}{d\Omega^2}[\Omega N(\Omega)]\ln\left|1 - \frac{\beta^2}{\Omega^2}\right| \tag{3}$$

and

$$g_3(\beta) = \int_0^\infty d\Omega \frac{d^2}{d\Omega^2}[\Omega N(\Omega)](\sqrt{\Omega+\beta} + \sqrt{|\Omega-\beta|} - 2\sqrt{\Omega}), \tag{4}$$

with $N(\Omega)=\{\exp(\Omega)-1\}^{-1}$. D is the diffusion constant and is deduced from $D=\mu\frac{kT}{e}$ with μ the electron mobility. The spin splitting of the conduction band contains the Zeeman term $g\mu_B H$, with $g=2.0$, and the *s-d* contribution $x_{eff}\alpha N_0 S B_S(T,H)$, αN_0 is the *s-d* exchange energy of 0.2 eV,[17] x_{eff} the effective mole fraction of the magnetic ions, and $B_S(T,H)$ the Brillouin function for $S=3/2$ for Co^{2+}. Thus, $\beta=[g\mu_B H + x_{eff}\alpha N_0 S B_S(T,H)]/kT$. The analytic expressions for $g_2(\beta)$ and $g_3(\beta)$ were given by Burdis and Dean[18] and Ousset *et al.*[19] In the simulation of positive MR, F_σ and x_{eff} are taken as fitting parameters.

The negative MR due to the field-suppressed weak localization can be expressed as follows:[11]

$$\Delta\sigma_N(H,T) = \sigma(H,T) - \sigma(0,T) = \frac{e^2}{2\pi^2\hbar}\left[\psi\left(\frac{1}{2}+y\right) - \ln y\right] \tag{5}$$

$$= \frac{e^2}{2\pi^2\hbar}\sqrt{\frac{eH}{\hbar}}f_3(y) \tag{6}$$

for two and three dimensions, respectively, where ψ is the digamma function, $y=\frac{\hbar}{4eHL_{Th}^2}$, and

$$f_3(y) = \sum_{n=0}\left[2(\sqrt{n+y+1} - \sqrt{n+y}) - \frac{1}{\sqrt{n+y+1/2}}\right]. \tag{7}$$

Here, L_{Th} is the dephasing length taken as a fitting parameter. The choice of two or three dimensions will be decided by relating the film thickness t and dephasing length L_{Th}, $t > L_{Th}$ for three dimensions and $t < L_{Th}$ for two dimensions.

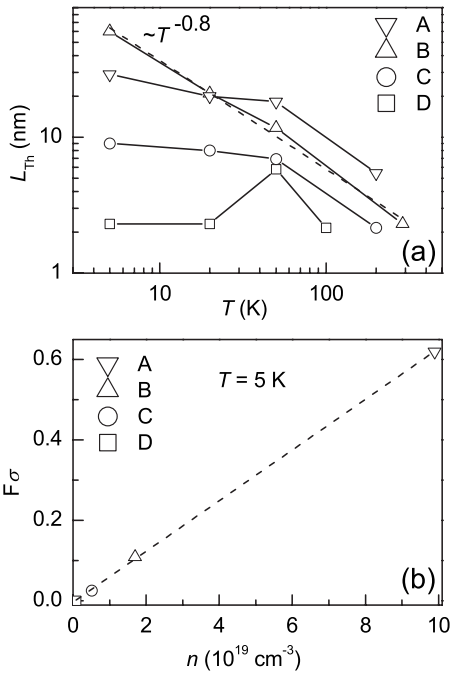

FIG. 3. (a) Temperature dependence of the dephasing length L_{Th} and (b) screening parameter for the Coulomb interaction F_σ at 5 K, for sample *A* (▽), sample B (△), sample *C* (○), and sample *D* (□) vs free electron concentration. The dashed line in (a) is fitting showing the dependence $T^{0.8}$ for sample *B*. The dashed line in (b) is the fitting showing the linear relationship between F_σ and n.

The total MR is a superposition of positive and negative MR, which can be calculated using

$$MR = \frac{\rho(H,T) - \rho(0,T)}{\rho(0,T)} = -\rho(H,T)[\Delta\sigma_P(H,T) + \Delta\sigma_N(H,T)]. \tag{8}$$

We first model the experimental MR of samples *A* ($k_F l=2.36$) and *B* ($k_F l=1.71$) in the weakly localized regime, as shown in Figs. 2(a) and 2(b). For sample *A*, due to the small thickness of about 26.5 nm, the corresponding two-dimensional equations had to be applied at 5 K and 20 K. At higher temperatures, positive MR has vanished. Fitting the data was performed only using Eq. (5) or (6), and L_{Th} was determined. The agreement between modeled and experimental MR data is excellent. Furthermore, we extended our model to Co-doped ZnO in the strongly localized regime, as shown in Fig. 2(c) for sample *C* ($k_F l=0.27$) and Fig. 2(d) for sample *D* ($k_F l=0.0065$). Also here the agreement between experimental and modeled data is very good. Table II lists the values of the fit parameters x_{eff}, F_σ, and L_{Th} for the samples under investigation. As expected the product of the Fermi wave vector k_F and mean free path l increases with increasing electron concentration and $k_F l$ approaches 1 in the weak localization region.[6] The parameters F_σ and L_{Th} exhibit a systematic dependence on electron concentration and temperature. The dephasing length L_{Th} decreases with increasing temperature and is much larger for samples in the weakly localized regime than for samples in strongly localized re-

gime. Figure 3(a) summarizes the temperature dependence of L_{Th} on a logarithmic scale. Only sample *B* shows the linear relationship. The fitting curve reveals a $T^{-0.8}$ dependence in close agreement with the $T^{-0.75}$ dependence observed in undoped *n*-ZnO.[6] The L_{Th} of sample *A* might be suppressed by the scattering at the top surface due to the small film thickness, as one can see that L_{Th} of sample *A* is larger than L_{Th} of sample *C* at high temperatures in three dimensions. The observed linear relationship between F_σ and the electron concentration, as shown in Fig. 3(b), illustrates that the free charge carrier concentration strongly influences the effective screening.

In summary, detailed MR investigations on Co-doped ZnO films in the weakly and strongly localized regime are reported. A large positive MR value of 124% has been observed in Co-doped ZnO with an electron concentration of 8.3×10^{17} cm^{-3} at 5 K, while only negative MR of −1.9% was observed in a Co-doped ZnO with electron concentration of 9.9×10^{19} cm^{-3}. The positive MR was modeled including the quantum correction on the conductivity due to the *s-d* exchange interaction induced conduction band splitting, while negative MR was modeled including the magnetic field suppressed weak localization. The theoretical explanation based on the combination of the positive and negative MR models well agrees with the experimental MR behavior in Co-doped ZnO.

This work was partially (Q.X., H.S., and H.H.) funded by BMBF (Grants No. FKZ03N8708 and No. CHN 05/010) and (L.H.) by DFG (Grant No. SCHM1663/1). The authors would like to thank G. Ramm for the target preparation and R. Schmidt-Grund and C. Sturm for ellipsometry measurements.

*Corresponding author. xuqingyu_1974@yahoo.com

[1] Ü. Özgür, Ya. I. Alivov, C. Liu, A. Teke, M. A. Reshchikov, S. Doğan, V. Avrutin, S.-J. Cho, and H. Morkoç, J. Appl. Phys. **98**, 041301 (2005).
[2] T. Dietl, H. Ohno, F. Matsukura, J. Cibert, and D. Ferrand, Science **287**, 1019 (2000).
[3] T. Fukumura, H. Toyosaki, and Y. Yamada, Semicond. Sci. Technol. **20**, S103 (2005).
[4] C. Liu, F. Yun, and H. Morkoç, J. Mater. Sci.: Mater. Electron. **16**, 555 (2005).
[5] F. Reuss, S. Frank, C. Kirchner, R. Kling, Th. Gruber, and A. Waag, Appl. Phys. Lett. **87**, 112104 (2005).
[6] T. Andrearczyk, J. Jaroszyński, G. Grabecki, T. Dietl, T. Fukumura, and M. Kawasaki, Phys. Rev. B **72**, 121309(R) (2005).
[7] Q. Xu, L. Hartmann, H. Schmidt, H. Hochmuth, M. Lorenz, R. Schmidt-Grund, C. Sturm, D. Spemann, and M. Grundmann, Phys. Rev. B **73**, 205342 (2006).
[8] Q. Xu, L. Hartmann, H. Schmidt, H. Hochmuth, M. Lorenz, R. Schmidt-Grund, C. Sturm, D. Spemann, M. Grundmann, and Y. Liu, J. Appl. Phys. **101**, 063918 (2007).
[9] N. Theodoropoulou, V. Misra, J. Philip, P. LeClair, G. P. Berera, J. S. Moodera, B. Satpati, and T. Som, J. Magn. Magn. Mater. **300**, 407 (2006).
[10] L. Hartmann, Q. Xu, H. Schmidt, H. Hochmuth, M. Lorenz, C. Sturm, C. Meinecke, and M. Grundmann, J. Phys. D **39**, 4920 (2006).
[11] P. A. Lee and T. V. Ramakrishnan, Rev. Mod. Phys. **57**, 287 (1985).
[12] R. Schmidt, B. Rheinländer, M. Schubert, D. Spemann, T. Butz, J. Lenzner, E. M. Kaidashev, M. Lorenz, A. Rahm, H. C. Semmelhack, and M. Grundmann, Appl. Phys. Lett. **82**, 2260 (2003).
[13] Y. Liu, Q. Xu, H. Schmidt, L. Hartmann, H. Hochmuth, M. Lorenz, M. Grundmann, X. Han, and Z. Zhang, Appl. Phys. Lett. **90**, 154101 (2007).
[14] P. P. Edwards, A. Porch, M. O. Jones, D. V. Morgan, and R. M. Perks, J. Chem. Soc. Dalton Trans. **2004**, 2995 (2004).
[15] M. Sawicki, T. Dietl, J. Kossut, J. Igalson, T. Wojtowicz, and W. Plesiewicz, Phys. Rev. Lett. **56**, 508 (1986).
[16] M. Csontos, T. Wojtowicz, X. Liu, M. Dobrowolska, B. Jankó, J. K. Furdyna, and G. Mihály, Phys. Rev. Lett. **95**, 227203 (2005).
[17] P. Kacman, Semicond. Sci. Technol. **16**, R25 (2001).
[18] M. S. Burdis and C. C. Dean, Phys. Rev. B **38**, 3269 (1988).
[19] J. C. Ousset, S. Askenazy, H. Rakoto, and J. M. Broto, J. Phys. (Paris) **46**, 2145 (1985).